1-1-2012

Thermally induced secondary atomization of droplet in an acoustic field

Saptarshi Basu

Abhishek Saha
University of Central Florida

Ranganathan Kumar
University of Central Florida

Thermally induced secondary atomization of droplet in an acoustic field

Cite as: Appl. Phys. Lett. **100**, 054101 (2012); https://doi.org/10.1063/1.3680257
Submitted: 22 September 2011 . Accepted: 06 January 2012 . Published Online: 01 February 2012

Saptarshi Basu, Abhishek Saha, and Ranganathan Kumar

Thermally induced secondary atomization of droplet in an acoustic field

Saptarshi Basu,[1] Abhishek Saha,[2] and Ranganathan Kumar[2,a)]
[1]*Indian Institute of Science, Bangalore 560012, India*
[2]*University of Central Florida, Orlando, Florida 32816, USA*

(Received 22 September 2011; accepted 6 January 2012; published online 1 February 2012)

We study the thermal effects that lead to instability and break up in acoustically levitated vaporizing fuel droplets. For selective liquids, atomization occurs at the droplet equator under external heating. Short wavelength [Kelvin-Helmholtz (KH)] instability for diesel and bio-diesel droplets triggers this secondary atomization. Vapor pressure, latent heat, and specific heat govern the vaporization rate and temperature history, which affect the surface tension gradient and gas phase density, ultimately dictating the onset of KH instability. We develop a criterion based on Weber number to define a condition for the inception of secondary atomization. © *2012 American Institute of Physics*. [doi:10.1063/1.3680257]

Interaction of fluid flow with an external acoustic field has been an important field of study for its wide range of applications in both micro and macro scales such as flame stability in combustion,[1] atomization and generation of liquid droplets,[2] and ultrasonic levitation.[3–8] Results have been reported on the generation of droplets from the long range capillary waves using ultrasound.[2,9–11] The physics of ultrasonic atomization of fuels in the presence of a surface tension gradient and temperature dependent properties is not treated in these studies, particularly for vaporizing droplets subject to significant external heating.

In this work, we study the thermal effects that lead to possible instability and break up observed in acoustically levitated fuel droplets. Our observations clearly illustrate that under certain conditions, heated droplets are susceptible to two distinct modes of instability: (a) short wavelength Kelvin-Helmholtz instability that pinches into satellite droplets at the equator but triggers no significant transient shape change and (b) long wavelength capillary wave instability that leads to significant variation in droplet aspect ratio and eventually to catastrophic breakup of the droplet. We report this unexpected finding that the temperature-dependent fuel properties and external heating rate may be exploited to provide insight into the relative strength of these two instabilities. Depending on the surface tension and viscosity gradients with temperature, either or both or no instabilities can occur in a droplet. Furthermore, the secondary atomization caused by short range pinching at the droplet equator always precedes the capillary waves that trigger bulk breakup, if both instabilities were to occur. We provide the criteria for the occurrence of such instabilities. Without external heating, no instabilities are observed throughout the entire lifetime of the droplet. In this paper, we focus on the first type of instability that can be observed at the droplet equator. The second type of instability of long wavelength will be discussed and explained in a subsequent article.

The current work uses a similar experimental setup described previously.[5–7] A 100 kHz acoustic levitator with amplitude of 156 dB (SPL) was used to suspend the droplets. The droplets were generated at the levitator pressure node using a micro syringe. A CO_2 laser with a beam diameter of 4 mm, lasing at 10.6 μm has been used to heat the droplet. The heating event has been recorded simultaneously by a high speed camera whose images were processed to obtain instantaneous diameter, aspect ratio, and shape changes and an infra-red (IR) camera to obtain the surface temperature of the droplet. Both cameras use microscopic lenses to increase the spatial resolution. The high speed camera was operated at 3000–10,000 fps, while the IR camera was operated at 100 fps.

Pure liquid droplets of four different fuels namely ethanol, diesel, kerosene, bio-diesel were levitated. The droplets had initial diameter of 500 ± 15 μm and were irradiated with 1.25 MW/m^2 heat flux. The radiative heating causes a sharp regression in droplet diameter (Figure 1) for the initial 0.2 s. The diameter reduction rate is fastest for ethanol, while kerosene, diesel, and bio-diesel vaporize slowly. The ethanol vapor pressure is higher (Table I) compared to the other three fuels, leading to a faster vaporization rate. The final surface temperature of the droplet (Figure 1) is analogous to the wet-bulb temperature of a vaporizing droplet in a hot gas medium and is low at the onset of heating; however, as the vapor pressure of the liquid increases with temperature, the evaporation rate increases. Faster vaporization progressively requires higher amount of latent heat thereby reducing the available sensible heat responsible for temperature rise. Maximum temperature is reached at equilibrium, which depends on the heating rate, vapor pressure, latent heat, and specific heat of the fuel. It is lowest (60 °C) for ethanol and highest (95 °C) for bio-diesel. Both kerosene and diesel exhibit maximum temperature of 80 °C.

After 0.3–0.4 s of heating, we observe different types of instabilities arising in kerosene, diesel, and bio-diesel droplets. These fuels start atomizing from the equator in the form of small droplets of sizes ~1–10 μm (Figure 2). This is a short wavelength instability that pinches tiny droplets at the equator. At the onset of this secondary atomization, the diameter reduction becomes a cumulative outcome of two events, i.e., evaporation and small scale atomization for all

a)Author to whom correspondence should be addressed. Electronic mail: ranganathan.kumar@ucf.edu.

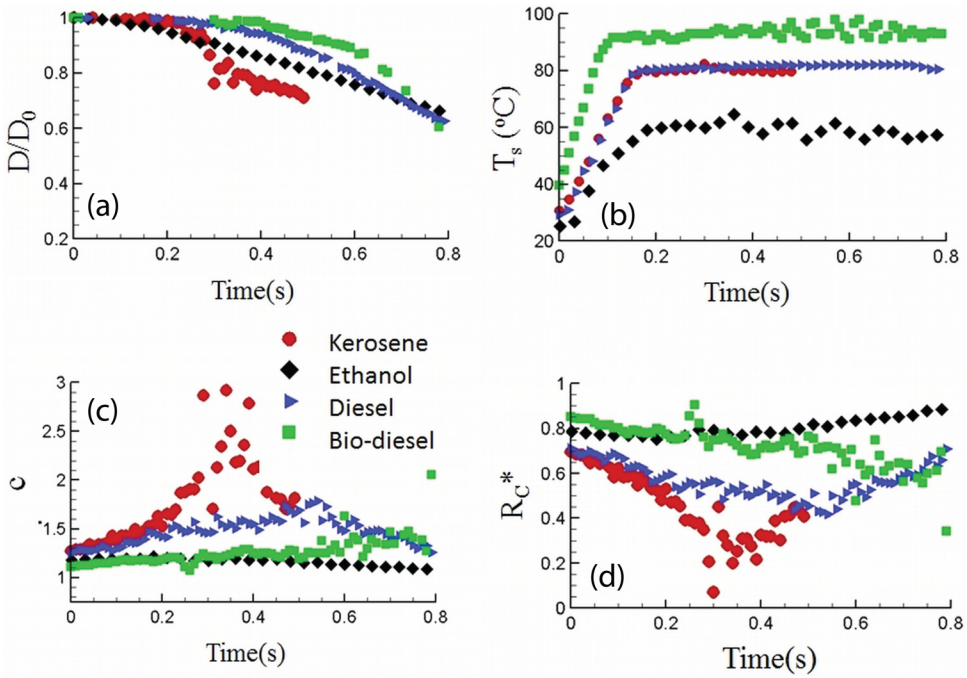

FIG. 1. (Color online) (a) Non-dimensional diameter (D/D_0), (b) average surface temperature (T_s), (c) aspect ratio, c and (d) non dimensional radius of curvature ($R_c^* = R_c/R$) for different fuels, R is equivalent radius of the droplet.

three fuels. Ethanol droplet, on the other hand, does not exhibit any atomization, hence the slower diameter reduction rate. We will discuss other events related to kerosene in the next article.

The classical Kelvin-Helmholtz (KH) type instability sets in when the relative motion between the levitated droplet and the surrounding air exceeds a critical value. This depends on the surface tension and density of the fluids[12]

$$u_{crit}^2 = [2(\rho_l + \rho_0)/\rho_l\rho_0]\sqrt{\sigma.(\rho_l - \rho_0).g}, \qquad (1)$$

where ρ_l and ρ_0 are densities of liquid and air, respectively, σ is surface tension, and g is acceleration of gravity. The relative velocity can be approximated by the acoustic streaming velocity u_{str}. For KH-instability, $u_{str} > u_{crit}$ condition has to be satisfied. In general the KH instability is the instability between gravitational force and shearing force due to relative motion between two fluid layers. In a levitated droplet, this can be extended to the instability between shear force due to acoustic streaming velocity at the droplet surface and net downward or upward force acting on the droplet, which can be scaled as "g" (gravitational acceleration). Although the net force may be different on the top and bottom sectors of the droplet, the critical condition always occurs near the equator as it has the smallest radius of curvature (explained later) and at this point the shear force due to streaming velocity (which is parallel to droplet surface) and the net gravitational force will act against each other leading to maximum instability. The acoustic streaming velocity is expressed as

$$u_{str} = P_0\gamma_0 Ma/\rho_0 c_0, \qquad (2)$$

where P_0 = atmospheric pressure, γ_0 = ratio of specific heats, ρ_0 = density of air stream around the droplet, c_0 = sonic velocity, Ma = acoustic Mach number. Mach number is directly related to the SPL (sound pressure level) of the levitator (constant for the current experiment) by $SPL[dB] = 197 + 20\log(Ma)$. Note that the heated, vaporizing droplet will always be covered with a concentrated fuel vapor blanket. Moreover, the acoustic streaming around the droplet suppresses the natural diffusion process of this concentrated vapor blanket. It is necessary to include the effect of this vapor blanket around the droplet while calculating the streaming velocity. From classical vaporization theory,[13] the mole fraction ($X_{l,s}$) and mass fraction ($Y_{l,s}$) of fuel vapor at the droplet surface can be calculated as

$$X_{l,s}(T_s) = \frac{P_{\text{sat}}(T_s)}{P_0}, \qquad (3)$$

$$Y_{f,s}(T_s) = \frac{X_{l,s}(T_s).W_l}{X_{l,s}(T_s).W_l + (1 - X_{l,s}(T_s)).W_{\text{air}}}, \qquad (4)$$

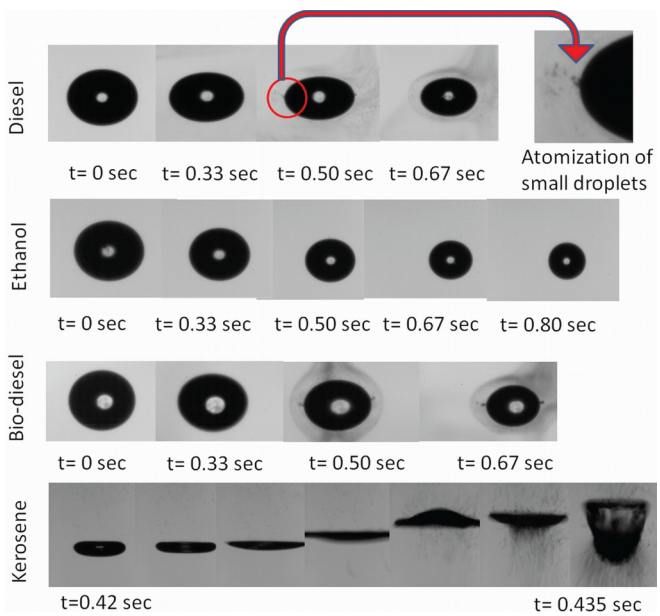

FIG. 2. (Color online) High speed images of atomization [diesel: atomization, biodiesel: atomization, Ethanol: no atomization] and stretching [Kerosene: stretching] of droplets (enhanced online). [URL: http://dx.doi.org/10.1063/1.3680257.1]

TABLE I. Temperature dependent property values for the fuels. T_s, surface temperature; σ, surface tension; μ, dynamic viscosity; P_{sat}, vapor pressure; ρ_l, liquid density; h_{fg}, latent heat.

	T_S (°C)[a]	σ (mN/m)[b]	$d\sigma/dT$ (mN/m/K)[c]	μ (cP)[b]	P_{sat}/P_{atm}[b]	ρ_l (kg/m^3)[d]	h_{fg} (kJ/kg)[d]
Kerosene	25–80	29.1–22.0	−0.117	1.82–0.85	4.33×10^{-3}–4.38×10^{-2}	790	322.2
Ethanol	25–60	22.5–19.4	−0.088	1.36–1.02	2.28×10^{-1}–6.15×10^{-1}	789	904
Diesel	25–80	31.6–23.9	−0.140	2.81–1.60	1.49×10^{-3}–1.13×10^{-2}	760	588.7
Bio-diesel	25–90	31.7–23.0	−0.123	4.60–1.70	4.49×10^{-9}–1.01×10^{-5}	787	254

[a]Initial and final temperature.
[b]Determined at initial and final temperature.
[c]Averaged over the temperature range observed during the experiment.
[d]At initial temperature.

where P_{sat} is vapor pressure of the fuel, T_s is the average surface temperature of the droplet, W_l and W_{air} are molecular weights of the liquid and air, respectively. The effective density of the vapor film around the droplet is

$$\rho_{0,\text{eff}}(T_s) = \left[\frac{Y_{f,s}(T_s)}{\rho_{l,\text{vap}}(T_s)} + \frac{1 - Y_{f,s}(T_s)}{\rho_{\text{air}}(T_s)}\right]^{-1}. \quad (5)$$

The streaming velocity can be redefined as

$$u_{\text{str-eff}} = \frac{P_0\gamma_0 Ma}{\rho_{0,\text{eff}}(T_s)c_0}, \quad (6)$$

which is a strong function of the vaporization characteristics of the different liquid fuels.

In general, the criterion for droplet atomization events is defined in terms of Weber number, which is the ratio of pressure force and capillary force. In acoustically levitated droplet, the Weber number, $We = 8P_B/P_\sigma$, is defined as the ratio of Bernoulli's stress (pressure) and stress due to surface tension,[11] where $P_B = 0.5P_0\gamma_0Ma^2$. The stress due to surface tension is given by $P_\sigma = 2\sigma/R$, where R is the droplet radius. Thus, $We = 2P_0\gamma_0Ma^2R/\sigma$. Using an effective Mach number

$$Ma_{\text{eff}} = u_{\text{str-eff}}/c_0, \quad (7)$$

$$We_{\text{eff}} = \frac{2P_0\gamma_0Ma_{\text{eff}}^2R}{\sigma} = \frac{2P_0\gamma_0(u_{\text{str-eff}}/c_0)^2R}{\sigma}. \quad (8)$$

We_{eff} is transient for a vaporizing droplet due to temperature dependent properties and fuel type. Without external heating, the effective Weber number exhibits dependence only on the droplet diameter and slow transient variations.

For KH instability, the critical Weber number for atomization is

$$We_{\text{crit}} = 2P_0\gamma_0(u_{\text{crit}}/c_0)^2R/\sigma. \quad (9)$$

Since the small scale atomization only occurs at the droplet equator, it is more appropriate to use R_c (radius of curvature at the droplet equator) as the length scale to redefine We_{eff} and We_{crit}. The aspect ratio of the droplet changes dynamically as heating and vaporization progress with time (Figure 1). The shape of the droplet approximates to an ellipse, and its local radius of curvature at any point on the equator perimeter is $r_c = (b^2\cos^2t + a^2\sin^2t)^{3/2}/a.b$; a and b are the major and minor axes, $c(=a/b)$ is the aspect ratio, and t is calculated by $\varphi(t) = \tan^{-1}(\frac{a}{b}\tan t)$. φ is the polar angle with the ellipse center as origin. For $\varphi = 0$ or $\pi/2$ the radius of curvature at the equator, $R_c = b^2/a = b/c$. The criterion for atomization can be recast as $We_{\text{eff}} > We_{\text{crit}}$, where $We_{\text{crit}} = 2P_0\gamma_0(u_{\text{crit}}/c_0)^2R_c/\sigma$ and $We_{\text{eff}} = 2P_0\gamma_0(u_{\text{str-eff}}/c_0)^2R_c/\sigma$. The liquid surface tension is a function of temperature, and the droplet size exhibits a transient regression with heating. This implies that We_{crit} and We_{eff} vary as $\sigma^{-1/2}$ and σ^{-1} during the droplet heating cycle, We_{eff} and We_{crit} will progressively decay as the droplet surface temperature increases, and the difference $(We_{\text{crit}} - We_{\text{eff}})$ can decrease until the atomization criteria is satisfied. Therefore, for liquid droplets with similar surface tension gradients, the probability of KH instability increases for higher surface temperature.

Initially, We_{crit} is larger compared to We_{eff} for all fuels (Figure 3). For diesel and bio-diesel, high speed images corroborate the time at which We_{eff} converges to We_{crit} and atomization is triggered. Kerosene reaches this condition fastest (around 0.3 s). In the absence of external heating, We_{crit} and We_{eff} would have exhibited a very slow change due to natural evaporation of the droplet. Thus, no atomization would be observed if there is no external heating. With heating, the vaporization pattern for each fuel droplet is different. The change in the temperature and diameter of a vaporizing droplet depends on the vapor pressure, latent heat and specific heat. The surface temperature and vapor pressure also dictate the change in vapor density around the droplet as explained earlier. Ethanol shows a low surface temperature, thereby reducing the possibility of KH instability.

In general, all droplets deform into an ellipsoidal shape and the oblateness or the aspect ratio is higher for the atomizing droplets (Figure 2). The theory of levitation[3,11] suggests that the aspect ratio is dependent on levitator SPL, surface tension, density, and droplet diameter. As mentioned earlier, the atomization occurs at the equator as it has minimum radius of curvature. For a given volume of droplet, the aspect ratio determines the radius of curvature at the equator. Parameters such as SPL and surface tension affect the aspect ratio and, in turn, affect the atomization. Increase in SPL and reduction in surface tension result in the augmentation of aspect ratio. However, both definitions of Weber numbers $(We_{\text{crit}} = 2P_0\gamma_0(u_{\text{crit}}/c_0)^2R_c/\sigma$ and $We_{\text{eff}} = 2P_0\gamma_0(u_{\text{str-eff}}/c_0)^2R_c/\sigma)$ use the radius of curvature as the length scale. So the change in SPL which alters the radius of curvature would have the same effect on both the Weber numbers and hence

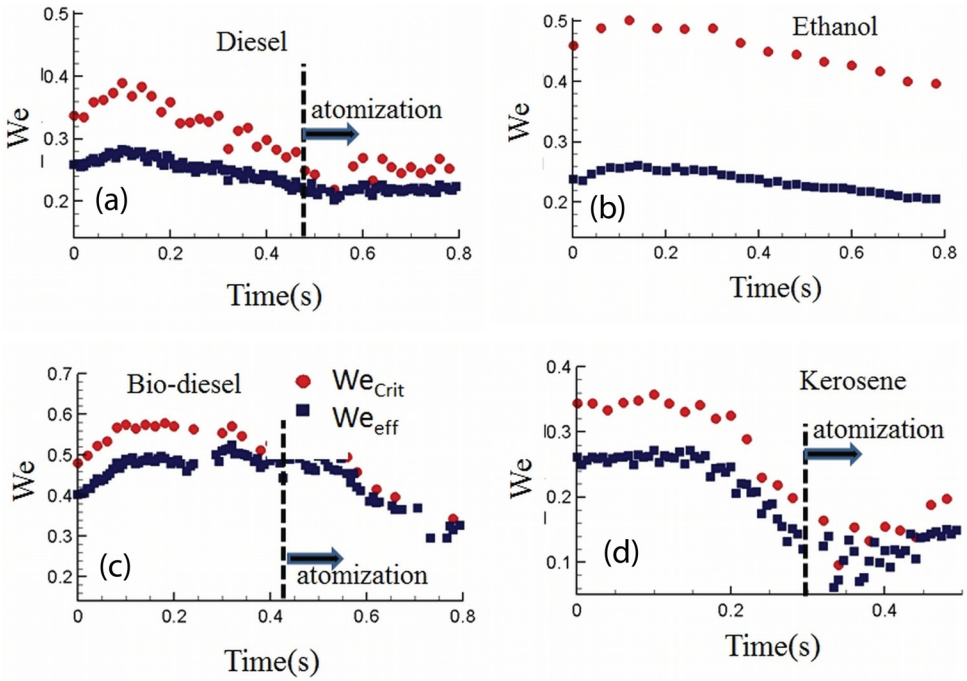

FIG. 3. (Color online) Critical Weber number (We_{crit}) and effective Weber number (We_{eff}).

would not change the instability criterion. On the other hand, the surface tension has separate and distinct effects on We_{crit} and We_{eff}. Change in surface tension would not only affect the aspect ratio but would also influence the Weber numbers directly. The change in aspect ratio (or radius of curvature) would create similar changes on both the Weber numbers as mentioned earlier. However, We_{crit} and We_{eff} show $\sigma^{-1/2}$ and σ^{-1}dependence. Surface tension decreases with temperature, leading to a sharper rise in We_{crit} than We_{eff}. It is difficult to conduct experiments with liquid droplet under external heating to demonstrate the effects of surface tension on KH instability, as the droplet will vaporize and create a vapor blanket around it, changing the streaming velocity and thereby altering We_{eff}. However, for liquids like kerosene (Figure 1), vaporization is not significant for the initial 200 μs, so the effect of the vapor blanket on streaming velocity would not be significant. Similarly, diesel also does not vaporize in the same duration, resulting in a sharp increase in temperature (up to 80 °C), which reduces its surface tension. In the first 100 μs (Figure 3(a)), We_{crit} and We_{eff} increase by ~20% and ~10%, respectively. The experiments were repeated a few times and were observed to be within 5%-10% of each other in terms of We_{crit} and We_{eff}, time of atomization and critical aspect ratio. Thus, the physics reported here is repeatable and sensitive only to the SPL of the levitator, properties of the fluid, and the laser heating rate. However, the SPL of the levitator and the laser power level were maintained constant for all fluids for all experimental runs. The uncertainty in We_{crit} and We_{eff} due to jitter in laser power and variation in the initial droplet diameter and SPL level of the levitator is negligibly small.

In summary, this analysis shows that the observed secondary atomization in levitated fuel droplets is primarily due to thermal effects. Since the density of fuels tested are very close to each other, properties such as vapor pressure, latent heat, and specific heat govern the vaporization rate and temperature history, which affect the surface tension gradient and gas phase density, ultimately dictating the onset of KH instability. High surface temperatures achieved in diesel, bio-diesel, and kerosene favor small scale atomization through KH instability. The temperatures for fuels like ethanol having high vapor pressure and high latent heat tend to remain rather low, leading to more stable droplets.

[1]T. Lieuwen, J. Fluid Mech. **435**, 289 (2001).
[2]A. Qi, L. Y. Yeo, and J. R. Friend, Phys. Fluids **20**, 074103 (2008).
[3]A. L. Yarin, M. Pfaffenlehner, and C. Tropea, J. Fluid Mech. **356**, 65 (1998).
[4]W. J. Xie, C. D. Cao, Y. J. Lü, Z. Y. Hong, and B. Wei, Appl. Phys. Lett. **89**, 214102 (2006).
[5]A. Saha, S. Basu, C. Suryanarayana, and R. Kumar, Int. J. Heat Mass Trans. **53**, 5663 (2010).
[6]R. Kumar, E. Tijerino, A. Saha, and S. Basu, Appl. Phys. Lett. **97**, 123106 (2010).
[7]A. Saha, S. Basu, and R. Kumar, "Particle image velocimetry and infrared thermography in a levitated droplet with nanosilica suspensions," Exp. Fluids (to be published).
[8]A. Saha, S. Basu, and R. Kumar, "Effects of acoustic-streaming-induced flow in evaporating nanofluid droplets," J. Fluid Mech (to be published).
[9]D. D. Lobdell, J. Acoust. Soc. Am. **43**, 229 (1968).
[10]A. V. Anilkumar, C. P. Lee, and T. G. Wang, Phys. Fluids A **3**, 2497 (1991).
[11]E. G. Lierke, Acust. Acta Acust. **88**, 206 (2002).
[12]S. Chandrashekhar, *Hydrodynamic and Hydromagnetic Stability* (Dover Publications, New York, 1981).
[13]W. A. Sirignano, *Fluid Dynamics and Transport of Droplets and Sprays*, 2nd ed. (Cambridge University Press, New York, 2010).